IEEE Access
Multidisciplinary | Rapid Review | Open Access Journal

Received 16 March 2023, accepted 17 May 2023, date of publication 25 May 2023, date of current version 1 June 2023.

Digital Object Identifier 10.1109/ACCESS.2023.3280061

RESEARCH ARTICLE

Energy Demand Model of Battery E-Buses for LPT: Implementation, Validation and Scheduling Optimization

ANDREA DI MARTINO, GAURI SHANKAR PRASAD, FEDERICA FOIADELLI, (Senior Member, IEEE), AND MICHELA LONGO, (Member, IEEE)
Department of Energy, Politecnico di Milano, 20156 Milan, Italy
Corresponding author: Andrea Di Martino (andrea.dimartino@polimi.it)

ABSTRACT The progressive conversion of conventional bus fleets into full-electric fleets have gained focus in recent years, instilled by awareness about the environment and significant trends of urbanization. Public transport operators in major cities worldwide have put efforts into fulfilling this change. However, an efficient electrification process is still a challenge for most operators. This paper aims to propose an E-Bus vehicle model that estimates the actual energy consumption. The proposed model is implemented on the case study of a real bus line for Local Public Transport (LPT) and considers all technical characteristics of the vehicle. Real-time input data are represented by real driving cycles of the actual bus fleet and slope profile of the line. Real-time input data allow to establish directly the influence on the energy consumed during real operations. As simulation results, the global energy consumption and battery State of Charge (SOC) are then computed for the whole daily service operations. The simulation results are validated with the real data available and several scenarios are then considered within the simulations. Based on the results obtained, further improvements are proposed and discussed aiming to optimize the utilization of bus fleet, regarding both vehicles scheduling and new charging solutions.

INDEX TERMS Charging infrastructure, electric bus, energy consumption, local public transport, state of charge, vehicle scheduling.

LIST OF ABBREVIATIONS

D	Derivative controller.
EB	Electric Bus.
EV	Electric Vehicle.
HVAC	Heating, Ventilation and Air. Conditioning.
I	Integral controller.
LPT	Local Public Transport.
OC	Opportunity Charging.
OEM	Original Equipment Manufacturer.
P	Proportional controller.
PD	Proportional Derivative controller.
PID	Proportional Integral Derivative controller.
PTO	Public Transport Operator.
SOC	State of Charge.
WLTP	Worldwide-harmonized Light-duty vehicles Test Procedure.

The associate editor coordinating the review of this manuscript and approving it for publication was Kuo-Ching Ying.

NOMENCLATURE

A	Frontal vehicle area.
$APP_{\%}$	Accelerator pedal position.
$BPP_{\%}$	Brake pedal position.
C_D	Aerodynamic drag coefficient.
C_b	Braking torque.
C_{loss}	Driveline torque losses.
C_m	Motor torque.
$C_{m,reg}$	Regenerative braking torque.
C_{net}	Net propulsive torque.
C_{rated}	Motor nominal torque.

E_{bat}	Nominal electrical energy capacity of the battery.
F_b	Total braking force.
F_{bd}	Disk friction braking force.
F_{in}	Inertia force.
$F_{t,net}$	Net tractive force.
K_r	Rolling resistance coefficient.
P_{aux}	Electric power absorbed by on-board auxiliary systems.
$P_{discharge}$	Total discharge power of the battery.
$P_{discharge,real/ideal}$	Real/ideal discharge power of the. battery.
P_{loss}	Internal power losses of the battery.
P_m	Electric motor power required by the propulsion system.
P_{rated}	Motor nominal power.
$I_{discharge}$	Battery discharging current.
R_{aero}	Aerodynamic resistance.
R_g	Gravitational resistance force.
$R_{internal}$	Internal battery resistance.
R_r	Rolling resistance.
V_{oc}	Open-circuit voltage.
a	Instantaneous vehicle acceleration.
f	Regeneration factor.
g	Gravity acceleration.
m	Total vehicle mass.
r_w	Wheel radius.
v	Instantaneous vehicle velocity.
η_m	Motor efficiency.
θ	Slope angle.
ρ_{air}	Air density
τ_g	Gear ratio.
ω	Angular motor speed.
$\omega_{reg,th}$	Threshold value of angular motor speed for regenerative braking torque.

I. INTRODUCTION

Decreasing environmental impact of human and industrial activities is pushing worldwide cities and local governments to put into practice a variety of solutions oriented to reduce the pollution in urban areas. Some of them regard directly the Local Public Transport (LPT), considering policies like the rearrangement of the service offered between urban and suburban areas or a zoning process [1]. But for sure, the most implemented solution regards the improvement in the electrification of vehicle fleet in LPT. Since the electrification is somehow intrinsic for railways or underground transportation systems, the main challenge is nowadays represented by the total conversion of LPT's road vehicle fleets to Electric Vehicles (EVs). This is mainly centered around the metropolitan areas of the world because of increasing trends in urbanization; in fact, it is expected a growth up to two-thirds of global population to be living around metropolitan areas [2]. Until recently, accepting this evolution has been difficult due to the high upfront investment and limited range of EVs. The technological advancement and several government policies have allowed a successful implementation of the transition to full-electric bus fleets in major cities. This global trend has been increasing substantially over the recent years, since most cities are looking for solutions to improve air quality and reduce CO_2 emissions. In fact, environmental pollution in large cities is approximately 20% due to the transportation system [3]. Consequently, the cities have been eager to step up their efforts in a complete and progressive renewal of LPT bus fleets. From the perspective of decarbonization, green public mobility has indisputable advantages; these go from the reduction of carbon emissions to the real possibilities for public administrations and Public Transport Operators (PTOs) to reduce operating and maintenance costs and offer a high-quality service to their customers. Achieving global decarbonization goals and transforming a city into a smart city are two intrinsically related goals.

This paper aims to develop a simulation model of energy demand for an Electric Bus (E-Bus or EB) able to estimate the energy requirements for the normal daily service operation. The paper is oriented to describe in details the methodology used, exploiting further developments with respect to the starting results obtained previously [4]. In particular, novelty of the present work is emphasized by the different simulation scenarios performed, through whose results the optimal utilization of bus vehicle fleet is reached. The vehicle model includes the vehicle parameterization and it is based on already existing local driving scenarios. A general overview and methodology of modeling the vehicle and energy demand developed in Simulink is provided, focusing on all the subsystems. The case study is represented by a real bus route served with E-Buses described by the technical characteristics of the vehicle and of the route. The model has been implemented on the route chosen and the simulation results validated on real data. The model can be also employed to assess some modifications on the charging operations and helps to evaluate a different daily vehicle schedule.

II. STATE OF THE ART

Electrification of LPT has faced immense challenges over the last decade. In a urban context, the opening of a railway rapid mass transit line can offer a significant reduction of pollutant of about 4% [5]. The most limiting factor is as obvious the great economic expenses related to the design and construction of such urban railway lines. Therefore, the focus must move to bus vehicles circulating into the LPT network [6]. Many advancements have been developed for technical requirements in E-Bus market, battery and technologies, designing new efficient charging infrastructure and planning processes in transport companies. The battery technologies have advanced quite significantly thus leading to lower the corresponding prices per kWh. Combined with the need of a CO_2-free environment, the whole industrial world has been moving at a rapid pace towards electrification. An efficient E-Bus system design has been discussed in academic literature in a quite extensive manner, with

significant contributions from a number of experts in automotive engineering, energy engineering, automotive Original Equipment Manufacturers (OEMs), and nevertheless from PTOs. In recent years, the development of smart charging solutions and decreasing battery prices have enabled local PTOs to proceed with the conversion of conventional vehicles into a full-electric bus fleet [7], [8].

The highly increasing demand of zero-emission public transport buses and competitive external pressure has enforced the E-Bus market growth. China currently represents the leader with 99% of global E-Bus fleet (about 460,000) in service [8]. The actual E-Bus market in Europe is still growing and taking up roots in several cities, which are transforming part of their network now served by EVs only. After beginning with redundant vehicles and prototype testing, the first dedicated bus routes were electrified as part of the ZeEUS project such as in Barcelona, Bonn and Munster [9]. The next level has been completed by the sub-network electrification, with E-Buses operated only along several lines. There are examples of European cities that have started employing their technology towards a practical implementation, promoting and inspiring several cities around the world to face this change. Some remarkable examples are Vienna, London, and Eindhoven, the first few cities in Europe to begin sub-network operations at very early stages [9], [10], [11]. A completely electric LPT bus network is the final goal and is being targeted in several cities across the continent. The rise of E-Buses in Europe still continues: after 2,210 electric buses in 2020, a further 3,282 electric buses - in each case excluding trolleybuses - were newly registered in 2021, with manufacturers competing for market shares. Among 14,990 new public buses registered in 2021 in the European markets, 59.4% are already equipped with alternative drives [12]. Lithium-ion battery pack prices-per-kWh reduced by 89% in 2021 if compared with 2010, a 6% drop from 2020. Based on historical trends, it has been predicted that average battery pack prices should be below 100 $/kWh by 2024. It is at this turning point that the OEMs would be able to produce and sell mass-market EVs being strongly competitive to internal combustion vehicles in some specific marketplaces [13].

Advancement in battery technologies have played a major role, as battery lifetime is one the main parameters considered by any PTO when planning a switch from conventional to E-Bus fleet. A battery is typically considered to have reached the end of life when it has less than 80% of its initial capacity, rather than being completely exhausted. The warranted end-of-life capacity is an important factor to consider, as the lower the capacity at the end of its life, the fewer miles a E-Bus can drive [7]. The battery life cycle can be improved by introducing new technologies like solid-state batteries, which provide high life cycle, low thermal degradation and low degradation due to charging cycles, since the electrolyte is solid if compared with Li-ion batteries [14].

Also charging infrastructure plays a very crucial role in E-Bus system design, since every vehicle needs battery charge at regular intervals. Depending on the charging frequency and the charging power, two concepts can be distinguished: depot charging and opportunity charging [11]. Depot charging is also used during longer dwell times throughout the day, in a very similar way to Diesel bus operating scheme. The depot charging idea empowers a centralization of infrastructure in the depot. Typically, vehicle demand is different during peak and off-peak hours, and thus the energy demand. This can be accommodated to charge the vehicles at the depot during off-peak hours. Due to the low range limit of most E-Buses, depot charging is not entirely sufficient to complete the daily operations requirements. Opportunity charging helps in such cases by on-route charging and thus extending the depot charging effectiveness. This solution is suitable for terminal stops due to longer dwell times. This makes the vehicle independent of the installed vehicle battery capacity. The design of opportunity chargers depends highly on the location and complexity of the construction of such infrastructure. So, the schedule planning of the E-Bus transportation system must account for frequent visits to charging terminals, ensuring proper duration of dwell times [15]. However, the E-Bus technology, charging infrastructure and vehicle scheduling depend on the local scenario. Thus, every PTO must adapt the electrification process to achieve the targets. The literature references regarding the topic of E-Bus transportation system and charging infrastructure are briefly collected in Table 1, where the main differences, paybacks and drawbacks with respect to the aim of the present work are underlined.

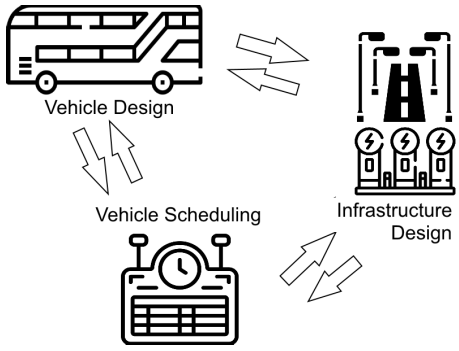

FIGURE 1. Interdependence of E-Bus system design processes.

III. GENERAL OVERVIEW

The service scheduling influences the technical design of vehicles and infrastructure and defines the entire framework of the scenario. This is established by the driving range and the dwell time duration at potential charging locations [11], [26], [27], [28], [29]. On the other hand, vehicle scheduling is limited by technical constraints of the E-Buses, such as limited battery capacity which decreases the operational range, and charging infrastructure, as depicted in Figure 1.

Vehicle scheduling is a fundamental aspect in operational planning as it focuses strongly on:

- costs, determining the vehicles purchase based on the required fleet size and the operational expenditure of the buses;

TABLE 1. Literature review for E-Buses topic.

Authors, year	Main scope	Method used	Paybacks	Drawbacks	Reference
Deb, 2022	Support Vector Machine based charging demand prediction of E-Buses	Machine learning	Quick results prediction	Large starting dataset, training required, no detailed vehicle specs needed, no scenario-dependant variablilty	[16]
Janjamraj et al. 2021	Refurbishment of existing conventional bus into an E-Bus	Numerical model/real tests	Numerical model exploited to update and electrify powertrain system of conventional buses	Light vehicle modelisation to assess the electric powertrain choice, Real on-route driving tests to determine the running parameters	[17]
Ashkezari et al. 2022	Opportunity charging system supplied by tramway DC line	Numerical model	Investigates the interactions between OC and DC tramway infrastructures when integrated	No vehicle model is analyzed	[18]
Beckers et al., 2021	On-line method for the future vehicle velocity and the energy consumption predictions of a E-Bus	Route discretisation, power-based vehicle model	A preliminary energy consumption prediction is derived from route characteristics and travel data	An inertial vehicle model is considered, no detailed vehicle specs used	[19]
Shihab et al., 2022	Reliability optimisation of E-Bus charging infrastructure and impact on electric grid	E-Bus model (scheduling and battery system)	Assessment of the charging infrastructure scheme based on bus operations, different scenarios	Focus on the infrastructure, no focus on vehicle fleet management	[20]
Rodrigues et al., 2020	Optimization framework for charging schedule at bus depots for both fuel buses and E-Buses	Mixed-Integer Linear Programming	Scheduling assessment based on charging routing operations	Focus on the charging/refueling schedule, no focus on vehicle	[21]
Zhang, 2017	Optimal configuration for an electrified bus route, the selection of appropriate E-Bus types (battery capacity) and recharging options to minimize the investment and operative costs	Mixed-Integer Linear Programming	Evaluation of different charging options based on bus operations	Vehicle model, traffic conditions and scheduling rearrangement are not considered	[22]
Zhang et al., 2017	Estimation of E-Bus charging load profile for a bus route and optimize electrification and sequence scheme model of city's bus routes	Particle Swarm Optimization	Minimization and planning of investments for charging infrastructure	No vehicle model implemented	[23]
Valenti et al., 2017; Liberto et al., 2018	Evaluation of changes in energy demand and pollutant emissions due to E-Buses, the electrification of both private and public transport fleet in urban area	Well-To-Well analysis	Evaluation of energy consumption, emissions and environmental impact from all stages of the value chain	No vehicle model implemented, no focus on scheduling and charging routing operations, specific emission/consumption functions implemented	[24], [25]
Present work	Evaluation of E-Bus energy consumption starting from actual bus route operations	Numerical e-Bus model	Vehicle technical specs considered, assessment of actual scheduling and SOC-based rearrangement, evaluation of OC solutions	No focus on the interactions between charging infrastructure and electric grid	-

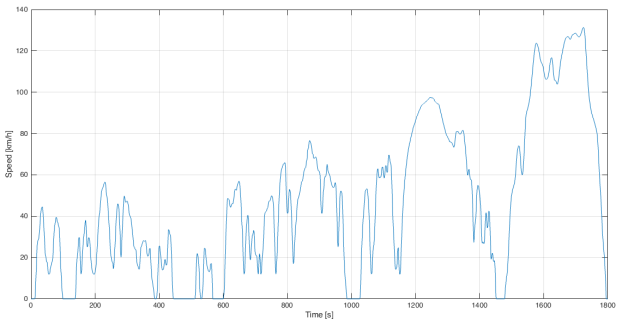

FIGURE 2. Example of normalized driving cycle (WLTP).

- maintenance scheduling, since vehicles must complete all inspections, complying with their maintenance plan [30], [31].

An efficient E-Bus design scheme must consider:

- the development of a mathematical model for a full-electric vehicle,
- an accurate modelisation of the energy consumption of E-Buses considering the route topology, weather conditions, and traffic flow, the operational requirements of power distribution networks,
- the optimal definition of the configuration for both on-board battery packs and chargers [32].

Therefore, a model for calculating E-Bus energy consumption on specific real routes has been created to evaluate the vehicle energy demand and infrastructure improvements. General data related to the existing local scenarios have been recorded through Phyphox phone application [33]. Since the energy demand depends on the route characteristics, as well as on the technical configuration of the vehicle, sampled dataset is constituted by the real-time speed profile and route elevation profile of the bus line considered. The actual standards prescribe to consider reference driving cycles to evaluate energy consumption, such as WLTP (Worldwide-harmonized Light-duty vehicles Test Procedure) in use in EU since 2015. These reference cycles provide the same testing conditions for different vehicles, thus leading to estimate the energy consumption for each and allowing a direct comparison between each other. Conversely, in this case a real driving cycles are acquired, thus to evaluate directly the impact of real operations on the overall energy consumption, considering both peak and off-peak periods during the day and among different days. In this way, the whole E-Bus system can be set up, meaning that not only the vehicle-related parameters but also the charging infrastructure can be designed optimally for the purposes.

IV. ENERGY DEMAND MODEL

The proposed model for the estimation of E-Bus energy consumption has been developed in Matlab-Simulink and considers a reference real driving cycle and the slope profile for the selected route as input data. A longitudinal driver block is implemented to process the input data. The characterization

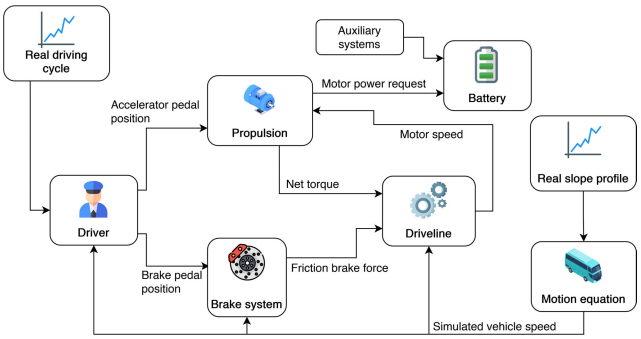

FIGURE 3. Energy demand model for Battery Electric Bus vehicle.

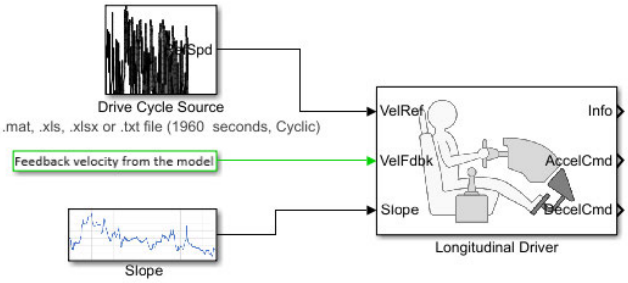

FIGURE 4. Longitudinal driver block.

of the vehicle considers propulsion, battery, braking and driveline subsystems [34]. The proposed Simulink model consists of 6 subsystems in total that describe the vehicle energy consumption and is graphically depicted in Figure 3.

A. LONGITUDINAL DRIVER BLOCK

The Longitudinal driver block implements a longitudinal speed-tracking controller. The model uses this block to model the response of a real driver, generating the commands necessary to track a longitudinal driving cycle. Based on the feedback of the simulated speed, acquired real-time slope and reference speed profiles, the block generates the dynamic normalized response of a driver, i.e. acceleration and braking pedal commands that can vary from 0 to 1. The block works as a Proportional Integral Derivative (PID) controller and adapts the acceleration and brake pedal position to follow the real bus speed profile. The choice to set a PID in spite that a PD or a simple P controller is based on the stability reached by such controller with respect to PD and P, which can generate unstable response. Moreover, since the simulation scenarios are based on real bus operations, it is meaningless to consider a normalized reference driving cycle. As aforementioned, these driving cycles are mainly designed to evaluate the energy consumption of different vehicles based on a standard framework. The inputs to the driver system block are shown in Figure 4.

B. BRAKE SYSTEM

The Brake system block computes the friction braking force as output, based on the brake pedal position coming from the Longitudinal driver block as input. The braking force

is computed and braking command is converted into the desired braking force, being known the tyre-road adhesion coefficient. Since the electric vehicle is capable to generate a braking action also by the electric motor, according to a regeneration braking factor, the desired brake force is then divided into two main components:

- the friction braking force developed by brake disks,
- the regenerative brake force developed by electric motor working as current generator.

Since the regenerative braking is not effective at low speeds, usually a threshold value is chosen in the range of $10 \div 25$ km/h. Below this threshold value, only friction braking force is applied, while above this threshold both friction and regenerative braking contributions are applied, as reported in (1) [35].

$$F_b = \begin{cases} BPP_{\%}\,(1-f)\,F_{bd} & \text{if } \omega > \omega_{reg,th} \\ \\ BPP_{\%}F_{bd} & \text{if } \omega \leq \omega_{reg,th} \end{cases} \tag{1}$$

where:

- $BPP_{\%}$ is the percentage of brake pedal position,
- F_b is the total braking force,
- F_{bd} is the disk friction braking force,
- f is the regeneration factor,
- ω is the actual angular motor speed,
- $\omega_{reg,th}$ is the threshold value of angular motor speed for regenerative braking torque.

C. PROPULSION SYSTEM

The accelerator pedal position provided by the driver block acts as an input also to Propulsion system block, which computes a corresponding positive torque for each time instant, as reported in Figure 5. Two working areas can be distinguished within the motor diagram, as depicted by Figure 5b:

1) Increasing motor power (or constant motor torque)
2) Constant motor power.

The constant motor torque value is computed according to this distinction and reported in (2). In particular, the motor torque analytical formulation is given as the minimum value between the two working conditions.

$$C_m = \min\left(C_{rated}; \frac{P_{rated}}{\omega}\right) \cdot \eta_m APP_{\%} \tag{2}$$

where:

- $APP_{\%}$ is the percentage of accelerator pedal position,
- C_m is the motor torque,
- C_{rated} is the motor nominal torque,
- P_{rated} is the motor nominal power,
- η_m is the motor efficiency,
- ω is the angular motor speed.

During starting phases, angular motor speed is very low ($\omega \to 0$), thus the value computed by $\frac{P_{rated}}{\omega} \to \infty$. This leads to consider a constant output motor torque. Conversely, when motor power is kept constant, motor torque starts to decrease due to increasing speed with a hyperbolic relation given by $C_m = \frac{P_{rated}}{\omega}$.

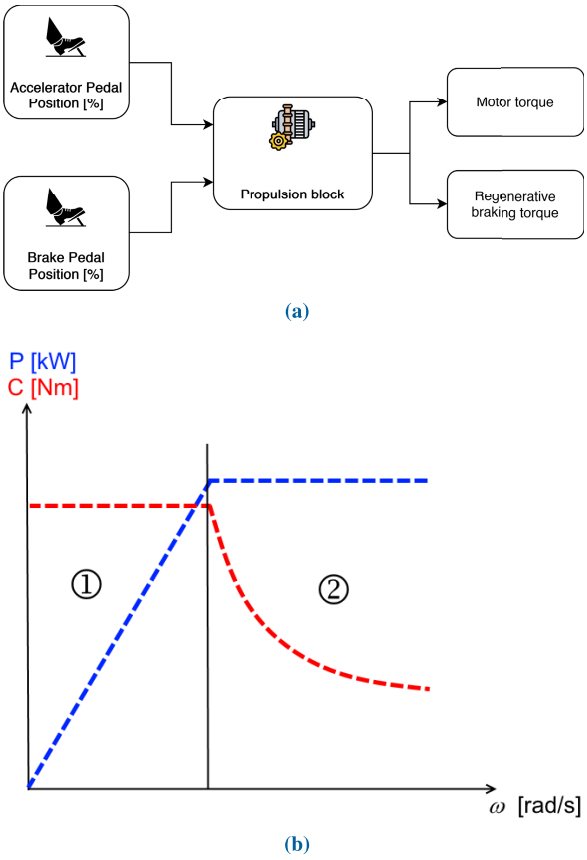

FIGURE 5. Propulsion system block for E-Bus vehicle model: (a) input and output variables and (b) motor diagram.

When braking phase is deployed, the corresponding $BPP_{\%}$ command becomes greater than zero while $APP_{\%} = 0$. Therefore, the propulsion block stops to compute the motor torque and generates only braking torque, whose analytical formulation is given in (3).

$$C_b = \begin{cases} BPP_{\%} \cdot f\,\tau_g C_{m,reg} & \text{if } \omega > \omega_{reg,th} \\ \\ 0 & \text{if } \omega \leq \omega_{reg,th} \end{cases} \tag{3}$$

where

- C_b is the braking torque
- $C_{m,reg}$ is the regenerative braking torque,
- τ_g is the gear ratio.

Net propulsive torque is obtained by subtracting braking torque from motor torque, according to (4).

$$C_{net} = C_m - C_b \tag{4}$$

where C_{net} is the net propulsive torque, either motor or braking.

The utility of (4) is related to account for the correct sign of either motor or regenerative braking torque in Longitudinal Vehicle Dynamics block. In particular, as previously

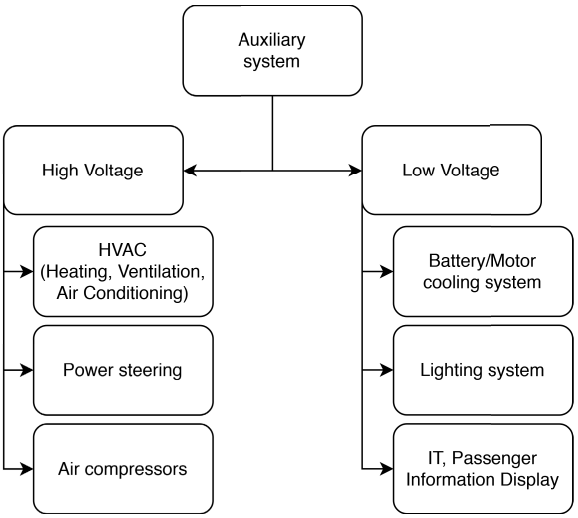

FIGURE 6. Auxiliary consumption.

remarked, only one between accelerator and brake pedals will be active, and therefore C_{net} will depend only on one single contribution of propulsion torque. The amount of electric motor power and the net motor torque transmitted to the driveline are the output of this block.

D. BATTERY SYSTEM

The Battery system block requires as input the total power of discharge $P_{discharge}$ reported in (5), as the sum of:

- the electric motor power required by the propulsion system P_m,
- the electric power absorbed by on-board auxiliary systems P_{aux}.

$$P_{discharge} = P_m + P_{aux} \tag{5}$$

On-board auxiliaries include several electrical components that are briefly summarized by Figure 6 and hereby listed:

- for high voltage auxiliaries
  - Power steering,
  - Air compressor,
  - Heating, Ventilation and Air Conditioning (HVAC) system.
- for low voltage auxiliaries
  - Lighting system,
  - Battery and motor cooling system,
  - Infotainment, Passenger Information Display.

The battery is represented by a real independent voltage source (or series-equivalent dipole) formed by:

- an ideal voltage source, defined as an open-circuit voltage V_{oc},
- the internal battery resistance $R_{internal}$.

According to (6), the real (or net) discharge power of the battery is equal to the difference between ideal discharge power and the battery losses, linked to its internal resistance.

$$P_{discharge,real} = P_{discharge,ideal} - P_{loss} \tag{6}$$

where:

- $P_{discharge,real/ideal}$ is the real/ideal discharge power of the battery,
- P_{loss} is the amount of internal power losses of the battery.

The battery $P_{discharge,ideal}$ is modeled according to the relationship reported in (7). Since the series-equivalent dipole is formed by the series of an ideal voltage source and the battery own internal resistance, the power losses are considered according to (8).

$$P_{discharge,ideal} = V_{oc} I_{discharge} \tag{7}$$

$$P_{loss} = R_{internal} I^2_{discharge} \tag{8}$$

Thus, it is possible to build up the main relationship stated in (6) with (7), (8) and it is possible to retrieve the discharge current according to the analytical solution of (6) as reported in (9).

$$I_{discharge} = \frac{V_{oc} - \sqrt{V_{oc}^2 - 4P_{discharge,real}R_{internal}}}{2R_{internal}} \tag{9}$$

where $I_{discharge}$ is the discharging current of the battery.

The battery State of Charge (SOC) can be evaluated according to (10) as a function of the rated energy capacity measured in kWh.

$$SOC_{batt} = \frac{-\int_0^T V_{oc} I_{discharge} dt}{E_{batt}} \cdot 100 \tag{10}$$

where E_{bat} is the nominal electrical energy capacity of the battery.

The SOC provides the current battery status expressed in percentage values where 0% indicates fully discharged and 100% indicates fully charged battery. In this model, to minimize battery degradation and ensure safe battery operation:

- the upper SOC limit is set to 80% of full battery charge,
- the lower SOC limit is set to 20% of full battery charge [36].

E. DRIVELINE SYSTEM

The net motor torque computed in Propulsion system, the friction brake force from the Brake system and the instantaneous simulated vehicle speed act as input data to the Driveline system block. The simulated vehicle speed is here used to estimate the amount of friction losses due to driveline. Starting from the net propulsive torque, the positive tractive force supplied by the driveline to the tires is calculated according to (11).

$$F_{t,net} = \frac{\tau_g}{r_w}(C_{net} - C_{loss}) - F_{bd} \tag{11}$$

where

- $F_{t,net}$ is the net tractive force,
- C_{loss} expresses the driveline friction losses as torque,
- r_w is the wheel radius.

The net tractive force delivered by the driveline and acting on the vehicle is the output of this block and acts as input for the Longitudinal vehicle dynamics block.

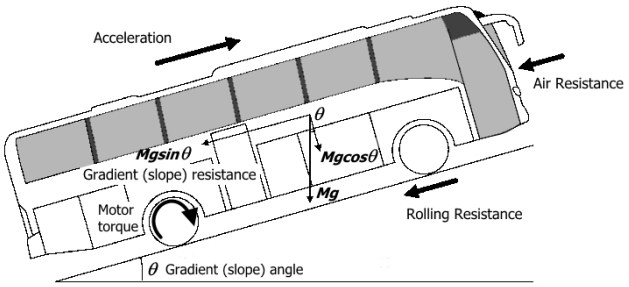

FIGURE 7. Longitudinal Forces on a bus in motion.

F. LONGITUDINAL VEHICLE DYNAMICS BLOCK

The Longitudinal Vehicle Dynamics block receives the net tractive force in input and compares it with the sum of motion resistances opposing the direction of motion. In every time step of the trip, as shown in Figure 7 the vehicle motion mainly depends on the following contributions:

- the rolling resistance R_r (12),
- the aerodynamic force R_{aero} (13),
- the resistance force due to the slope R_g (14),
- the inertia force F_{in}, for which the maximum vehicle mass is considered (15).

$$R_r = K_r mg\cos\theta \tag{12}$$

$$R_{aero} = \frac{1}{2}\rho_{air} C_D A v^2 \tag{13}$$

$$R_g = mg\sin\theta \tag{14}$$

$$F_{in} = ma \tag{15}$$

where:

- m is the total vehicle mass,
- g is the gravity acceleration,
- K_r is the rolling resistance coefficient,
- ρ_{air} is the air density,
- C_D is the aerodynamic drag coefficient,
- A is the frontal area of the vehicle,
- v is the instantaneous vehicle velocity,
- a is the instantaneous vehicle longitudinal acceleration,
- θ is the instantaneous slope angle.

Therefore, this system calculates the acceleration of the vehicle and, consequently, the simulated speed according to (16) that describes the longitudinal vehicle motion.

$$a = \frac{F_{t,net} - \left(R_r + R_{aero} + R_g\right)}{m} \tag{16}$$

Both physical quantities v, a are then fed back to Longitudinal driver, Brake system and Driveline blocks, useful to perform internal calculations for subsequent simulation steps.

V. CASE STUDY: A REAL BUS ROUTE

The vehicle model has been tested and validated on a reference route. Then, simulation runs have been performed based on the reference route chosen. The case study considers a real route in Northern Italy already served by E-Buses. The route

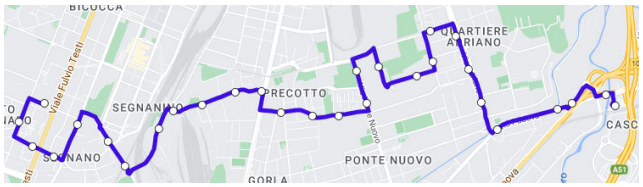

(a)

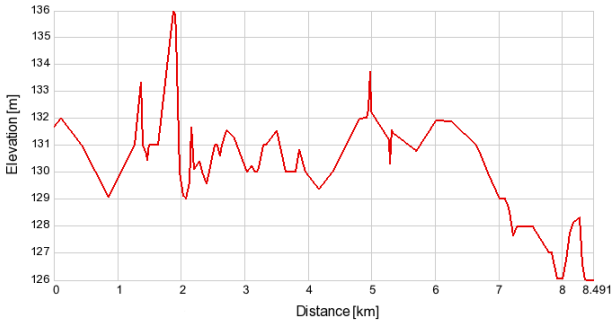

(b)

FIGURE 8. Bus route considered, 29 stops, length 8.5 km: (a) map and (b) altitude profile.

is 8,5 km long and depicted in Figure 8a, while Figure 8b depicts the altitude profile of the route considered from which the slope profile is derived through numerical way.

For this specific bus route, speed and altitude profiles have been recorded for various roundtrips at different hours of the day and different days of the week using Phyphox mobile application [33]. The need to have real data instead of generalized data is due to the fact that the evaluation of energy demand here depends on the operating and route characteristics as well as on the technical configuration of the vehicle. A valuable option is to consider a measurement campaign in which every eligible bus is operated under worst-case conditions on the selected bus route. However, such a test operation would lead to increase the operative costs and furthermore, worst-case service conditions are not present throughout the year. Hence, measurement data are collected from existing bus route operations and processed into a local scenario through the numerical model. The use of generalized and averaged data (as normalized driving cycles) could in this case affect the final results excluding the most significant influences. The major challenge here is to identify the energy demand-affecting parameters, as for example the speed profile. Therefore, the actual speed profile from real operations as well as the slope of the route served and selected are sampled.

The services are characterized by peak and off-peak hours related to working and weekend days. The service peak hours are 7:00 to 9:00 AM and 5:00 to 7:00 PM. The bus service and energy consumption depend on the daily period of service, with sensible variations among them. Figure 9a depicts the velocity profile related to a working day service-peak hour, while Figure 9b represent the same information acquired

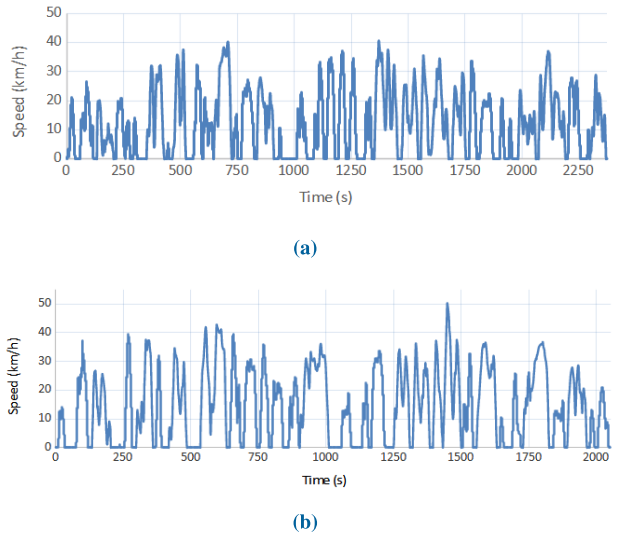

FIGURE 9. Speed profiles of a working day service: (a) peak hour, (b) off-peak hour service.

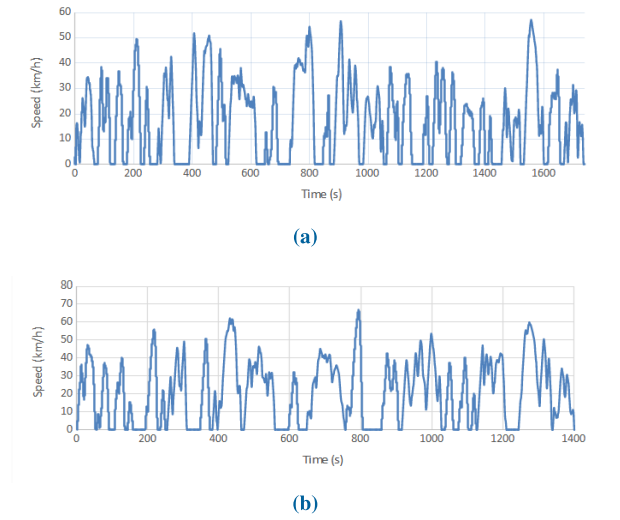

FIGURE 10. Speed profiles of a weekend day service: (a) peak hour service, (b) off-peak hour service.

for off-peak hours on working day. For weekends service, Figure 10a depicts the velocity profile for the peak hours whereas Figure 10b reports the same for off-peak hours.

It can be observed that as far as the speed profiles are concerned, during off-peak services the maximum speed is about 70 km/h for weekends whereas on working days it reaches only 50 km/h. Moreover, the dwell times vary a lot and are smaller for the weekends. Comparing peak hours, the maximum speed reached by the bus is respectively 55 and 40 km/h for weekends and working days, dwell times at stops are larger during peak hours of working days while dwell times at terminal stops are larger in peak hours of weekend services. These variations have a great impact on the energy consumption of the E-Bus. In addition to vehicle, motor, battery specifications and speed and altitude profiles, also several other simulation parameters depending on the driving

TABLE 2. Simulation parameters.

Parameters	SI unit	Value
Tyre-road adhesion coefficient	[-]	0.85
Regenerative braking threshold velocity	[km/h]	15
Regenerative braking factor	[-]	0.7
Air density	[kg/m^3]	1.23
Aerodynamic drag coefficient	[-]	0.79
Rolling resistance coefficient	[-]	0.01
Gravity acceleration	[m/s^2]	9.81
Total vehicle mass	[kg]	19000
Auxiliary energy consumption	[kWh/km]	1.41

conditions are required for the model set-up and are listed in Table 2 [37], [38], [39], [40], [41].

The simulation model assumes a dry tyre-road adhesion coefficient, since real data were recorded on dry weather conditions [40]. As aforementioned, the model implements a parallel braking system based on a direct combination between friction-based and regenerative braking torques. Regenerative brake factor represents the percentage of braking force delivered by regenerative braking. The regenerative braking threshold velocity is set at 15 km/h [38]. Aerodynamic drag and rolling resistance coefficients have been chosen and set according to [40]. Although various factors affect the energy consumption of a E-Bus trip, the average energy consumption rate of 1.41 kWh/km has been considered for auxiliary systems, which is based on the results obtained by employing E-Buses in a regular city bus route under a real-world evaluation experiment [41]. The relatively high value of auxiliaries energy consumption chosen allows to stress the simulation scenario for the output results provided by the vehicle model. Simulations are run through the model and prompt the energy discharged by the motor, the regenerated energy, and battery SOC. For every simulation, one roundtrip data has been considered with 4 minutes of dwell time at the terminal stop as an average of the acquired data.

VI. MODEL VALIDATION

During the day, the buses run in service during both peak and off-peak hours, thus the daily energy demand can be simulated using a combination of these roundtrip simulations. This information can be used to determine the daily energy demand from the buses for this route and thus, suggest any modification to the service if required for the improvement of the operations from feasibility, efficiency and financial point of view. In order to validate the data obtained from the developed model, real data of the E-Buses operating on the route among five working days have been recorded. The data referred to each bus in daily operations consists of:

- Bus number,
- Date of service,

TABLE 3. Prepared test data for validation.

Bus no.	Start of service [hh:mm:ss]	End of service [hh:mm:ss]	Discharged energy [kWh]	Regenerated energy [kWh]	Battery used [%]
EB-1	09:39:00	12:23:00	61	15	26
EB-2	06:12:00	10:18:00	90	20	37
EB-3	12:45:00	22:16:00	208	49	59
EB-4	16:43:00	19:52:00	65	15	16
EB-5	05:47:00	10:03:00	91	21	26
EB-6	13:03:00	20:07:00	151	38	45

TABLE 4. Prepared simulation scenarios of test data.

Bus no.	Service duration [min]	No. of Peak Roundtrips	No. of Off-peak Roundtrips	Duration on-line [min]	Duration off-line [min]
EB-1	164	0	2	145	19
EB-2	246	1	2	227.75	18.25
EB-3	571	2	5	528	43
EB-4	189	2	0	165.5	23.5
EB-5	256	2	1	238	18
EB-6	424	2	3	383	41

- Start of service time,
- End of service time,
- Discharged energy,
- Regenerated energy,
- Battery SOC.

These data were collected at depot before and after the service. Also the time of exiting from and returning to the depot has been considered. To simplify the process, test data have been prepared as shown in Table 3 based on the choice of six relevant bus services. Thus, from EB-1 to EB-6, the start and end of the service times cover the service durations of each bus running on working days. The discharged energy, regenerated energy and battery used test-data have been prepared by averaging the data of all the buses for 5 days that correspond to the similar duration of service and number of peak and off-peak roundtrips taken.

For the prepared test data, simulation scenarios have been created as shown in Table 4 based on the combination of peak and off-peak roundtrips during their service time. Duration on-line corresponds to the time spent in running along the path specified for the route. Duration off-line corresponds to the time spent in dwelling at the initial stop after each roundtrip and the time spent to reach the initial stop from the depot and going back to the depot itself after the last roundtrip.

After performing simulations based on the six EBs selected, the simulation results have been compared with the test data and depicted in Figure 11.

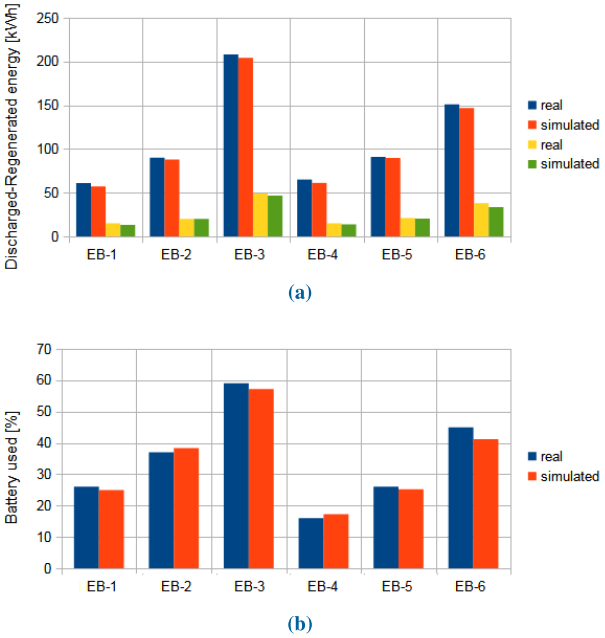

FIGURE 11. Error between real and simulated data: (a) discharged and regenerated energy, (b) Battery used.

The simulation results are close to the test data with mean errors within 3-6% for discharged energy, regenerated energy and battery used data. The sources of error are related to unavailable velocity profiles and driving behavior for the off-line duration paths. Moreover, the simulation data are obtained as a combination of roundtrips that belong either to peak hours or off-peak hours, whereas in reality there are few roundtrips which lie both in peak and off-peak region. Hence, since minimal errors emerged after data comparison phase, the model is meant as validated.

VII. RESULTS AND DISCUSSION

The model hereby presented has been then used to simulate the running behaviour of an EB running during a whole day of observation according to two distinct scenarios:

1) starting from real driving cycle data,
2) following the own timetable of the route considered.

A. REAL DRIVING CYCLE DATA

Simulations are run starting from real driving cycles acquired and reported in Figures 9, 10 as input data. The observations from the simulation results are shown in Table 5 for both the working days and weekends. In this way, it is possible to appreciate the difference between the two working conditions of an E-Bus.

As it can be observed, on working days the energy discharged is higher during peak hours as more time is spent to cover the same distance. On weekend days, a higher energy consumption is observed as the vehicle reaches higher maximum speeds for longer durations. In particular, off-peak shifts show higher energy discharged due to the higher maximum speed reached. Higher regeneration percentage is observed

TABLE 5. Roundtrip simulation results – working and weekend days.

	Roundtrip duration [s]	Discharged energy [kWh]	Regenerated energy [kWh]	[%]	Battery SOC [%]
		Working days			
Peak	4965	30.67	6.89	22.46	91.38
Off-peak	4353	28.65	6.75	23.56	92
		Weekend days			
Peak	3631	38.61	11.89	30.80	90.31
Off-peak	3217	41.38	13.58	32.81	89.92

during off-peak hours in both day types, because with higher speeds the duration of braking is longer and stronger than in the cases of peak hours: this leads to higher regeneration of kinetic energy available. Moreover, the lower maximum speed reached in peak hours on working and weekend days allows to regenerate a smaller amount of kinetic energy by the electric motor if compared with weekend days service operations. During roundtrips, energy consumption is about 8-11% of battery nominal capacity, being higher during peak hours of working days and off-peak hours on weekend days. It can be concluded that an E-Bus can cover 8-10 roundtrips along the route considered with a fully charged battery.

B. TIMETABLE SCENARIO

The model estimates the battery SOC used for each EB running, according to the initial timetable set for the bus route. Based on the simulation results, also additional considerations related to vehicle scheduling can be proposed. Timetable and results of the first simulation run are reported in Table 6.

It can be observed that EBs n° 1, 2, 3, 5, 6, 7, 8 have a substantial amount of battery left after the end of their service in the morning. Moreover, observing the service scheduling, it has been found that EBs n° 1, 2 and 5 stay in the depot while others are employed on services, also on other routes. Thus, based on the information about the start and end of service times, a modification could be performed by replacing EBs n° 11, 12 and 16 with 2, 5 and 1 respectively with their remaining battery SOC after the first service scheduled. This solution is proposed since service duration of EBs n° 1, 2, 5 do not overlap with each other. Having rearranged the scheduling service, a second simulation run can be performed to assess the new solution, considering the continuity of SOC between two subsequent services. The battery SOC simulations results have been listed in Table 7.

According to the results of the second simulated service, the remaining SOC for each bus is well above 20%, previously set as the lower limit for the battery. Thus, the proposed re-scheduling is both feasible and profitable as three buses were removed from the service. These EBs could then be used to provide services on other routes if needed.

TABLE 6. Battery Status for buses.

Bus no.	Start of service [hh:mm:ss]	End of service [hh:mm:ss]	Battery SOC [%]	Battery used [%]
1	05:23:00	12:49:00	58.83	41.17
2	05:32:00	09:48:00	74.81	25.19
3	05:47:00	10:03:00	74.81	25.19
4	05:57:00	09:30:00	82.8	17.2
5	06:04:00	10:00:00	61.68	38.32
6	06:12:00	10:18:00	61.68	38.32
7	06:25:00	13:23:00	58.83	41.17
8	06:34:00	13:36:00	58.83	41.17
9	06:37:00	13:08:00	58.83	41.17
10	09:39:00	12:23:00	75.09	24.91
11	09:49:00	12:35:00	75.09	24.91
12	12:11:00	19:34:00	58.83	41.17
13	12:45:00	22:16:00	42.84	57.16
14	12:49:00	21:58:00	42.84	57.16
15	13:03:00	20:07:00	58.83	41.17
16	13:10:00	21:20:00	50.83	49.17
4	13:22:00	22:12:00	42.84	57.16
17	16:14:00	21:41:00	66.82	33.18
9	16:43:00	19:52:00	82.8	17.2
18	17:17:00	20:19:00	82.8	17.2

TABLE 7. Battery SOC simulation results after re-scheduling.

Bus no.	Start of service [hh:mm:ss]	End of service [hh:mm:ss]	Battery SOC [%]	Battery used [%]
1	05:23:00	12:49:00	58.83	41.17
2	05:32:00	09:48:00	74.81	25.19
5	06:04:00	10:00:00	61.68	38.32
2	09:49:00	12:35:00	58.84	15.97
5	12:11:00	19:34:00	20.51	41.17
1	16:14:00	21:41:00	25.65	33.18

The numerical model presented shows strong potentialities to support numerically the proposal of a modification in the usual fleet scheduling, starting from the results obtained by the actual configuration. In addition, as a consequence of the numerical analysis, the energy demand model here developed can be exploited also to increase the effectiveness of electrification process planning.

C. IMPLEMENTATION OF OPPORTUNITY CHARGING

As a consequence of the analysis shown in Table 7, simulation results point out that EB-4 runs for two services and the service duration of EB-10 lies between the two services of EB-4. After the very first rearrangement, it was

TABLE 8. Battery SOC without Opportunity Charging.

Bus no.	Start of service [hh:mm:ss]	End of service [hh:mm:ss]	Battery SOC [%]
Service 1	05:57:00	09:30:00	82.80
Service 2	09:39:00	12:23:00	66.83
Service 3	13:22:00	22:12:00	9.67

TABLE 9. Battery SOC with Opportunity Charging.

Bus no.	Start of service [hh:mm:ss]	End of service [hh:mm:ss]	Battery SOC (+OC) [%]
Service 1	05:57:00	09:30:00	87.03
Service 2	09:39:00	12:23:00	75.29
Service 3	13:22:00	22:12:00	32.94

found that just replacing EB-10 with EB-4 would not be sufficient, since the remaining SOC of EB-4 after three services would lie below the SOC lower limit as reported in Table 8.

So, a possible solution to this critical point can be represented by the implementation of Opportunity Charging (OC) infrastructure. This solution is not present on the bus route considered but it can be derived from 200 kW pantographs chargers already installed on other routes. The implementation of OC has been performed for EB-4 as a case study in order to remove EB-10 from schedule. This solution has been then implemented into the simulation, considering 4 minutes of dwell time at the terminal stop, with the following partition:

- 1 minute for charging connection/disconnection,
- 2 minutes for charging operation at 200 kW constant nominal power.

The simulation has been carried out separately for the three services and results are shown in Figure 12a for the Service 1, Figure 12b for Service 2 and Figure 12c for Service 3 respectively as depicted in Table 9.

As prompted by the new updated scenario in Figure 12, with OC solution implemented, each EB starts the subsequent service with the remaining SOC from the previous service accomplished. Therefore, EB-4 starts its daily service with 100% fully charged battery and undergoes two OCs (red-circled), ending its service with a SOC equals to 87.03%. The second daily service is then accomplished after two OCs with a battery SOC of 75.29%. The last and longer daily service is executed and completed with 7 OCs and a remaining SOC equal to 32.94%. As reported in Table 9, EB-4 can provide three services with OCs with more than 30% of battery SOC remaining at the end of last service. With careful observations from the output results provided by the E-Bus model with implementation of OC solutions, 4 buses have been removed from the daily service of the route. Thus, a similar approach can be adopted also for other bus lines, thus improving the

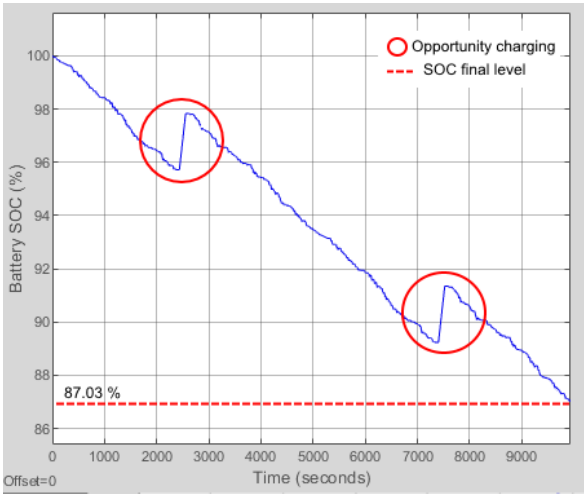

(a)

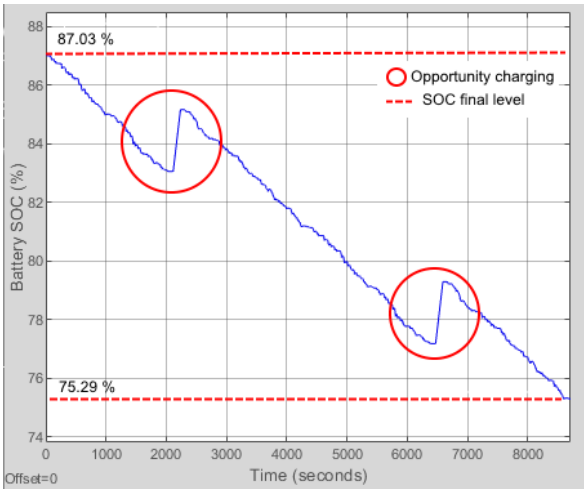

(b)

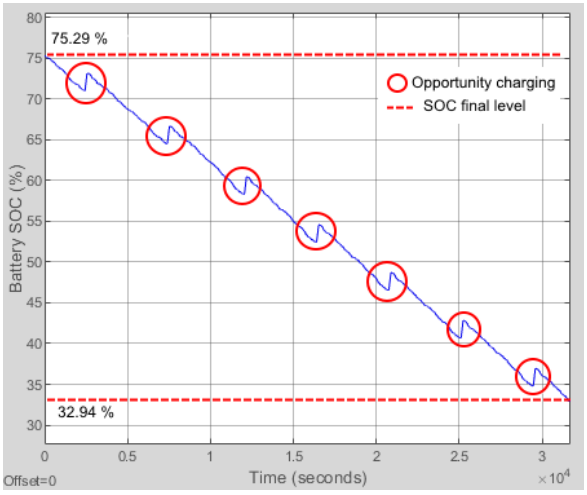

(c)

FIGURE 12. EB Simulations with Opportunity Charging for (a) service 1, (b) service 2, (c) service 3.

efficiency of the vehicle scheduling. Moreover, the daily public transport services can be provided with a lower number

of vehicles than the actually used. In this way, buses that have been removed from the schedule can be destined to serve other critical bus lines, thus helping to sustain the passenger demand and to increase route capacity.

VIII. CONCLUSION

An energy demand model for E-Buses was developed in Matlab-Simulink to preliminary evaluate the vehicle energy consumption during normal service operations. The modelisation of each vehicular subsystem of interest was provided, with particular focus on propulsion and battery energy storage. A longitudinal driver model was introduced as a PID controller, in order to replicate the driving cycle of a real bus driver, sampled through Phyphox mobile app. The model was then validated on available real data from daily service, proving to replicate effectively the real behaviour of the vehicle with minimal errors. As an unexpected payback, the output results provided made possible to re-schedule the service, thus optimizing the vehicle utilization and fleet SOC management. The capability of the model are emphasized through the assessment of smart charging solutions based on the energy requirement of the vehicle in service on the chosen route. Moreover, this work provides how a numerical vehicle model can act as a tool to help the electrification planning for an existing LPT network and can be implemented for analyzing any route served with conventional buses. It helps to estimate the energy demand of an equivalent E-Bus and provides help in both the evaluation of vehicle type and number for starting their services. For future developments, similar studies can be extended to other non-electrified routes of the network served with conventional vehicles, thus improving the actual vehicle scheduling of the route. An efficient electrification can be carried out to achieve the target of full-electric conversion of the fleet.

REFERENCES

[1] R. Borck, "Public transport and urban pollution," *Regional Sci. Urban Econ.*, vol. 77, pp. 356–366, Jul. 2019, doi: 10.1016/j.regsciurbeco.2019.06.005.

[2] Enel. (2021). *Enel X Strategies for Public Transport: Electrification Carries the Need for Innovative Solutions*. Accessed: May 19, 2022. [Online]. Available: https://www.sustainable-bus.com/news/enel-x-public-transport-electric-bus/

[3] R. Capata, "Urban and extra-urban hybrid vehicles: A technological review," *Energies*, vol. 11, no. 11, p. 2924, Oct. 2018, doi: 10.3390/en11112924.

[4] A. Di Martino, M. Longo, G. S. Prasad, F. Foiadelli, W. Yaici, and D. Zaninelli, "Implementation and validation modelling of energy demand of electric buses for local public transport," in *Proc. 10th Int. Conf. Smart Grid (icSmartGrid)*, Jun. 2022, pp. 266–270, doi: 10.1109/icSmartGrid55722.2022.9848756.

[5] N. Gendron-Carrier, M. Gonzalez-Navarro, S. Polloni, and M. A. Turner, "Subways and urban air pollution," Nat. Bur. Econ. Res., Cambridge, MA, USA, Tech. Rep. 24183, Jan. 2018, doi: 10.3386/w24183.

[6] M. Abbasi, "Study of electric buses and their impact on the environment in urban networks," Feb. 2018.

[7] A. O'Donovan, J. Frith, and C. McKerracher. (Apr. 2018). Electric buses in cities: Driving towards cleaner air and lower CO_2. Bloomberg New Energy Finance. Accessed: May 22, 2022. [Online]. Available: https://about.bnef.com/blog/electric-buses-cities-driving-towards-cleaner-air-lower-co2/

[8] P. Cazzola, M. Gorner, J. Tattini, R. Schuitmaker, S. Scheffer, L. D'Amore, H. Signollet, L. Paoli, J. Teter, and T. Bunsen, "Global EV outlook 2019—Scaling up the transition to electric mobility," Int. Energy Agency, Jun. 2019. [Online]. Available: https://www.oecd-ilibrary.org/content/publication/35fb60bd-en, doi: 10.1787/35fb60bd-en.

[9] P. Bruge, "ZeEUS launch in Bonn: Six e-buses to commence regular service," UITP, Brussels, Belgium, Tech. Rep., 2016.

[10] M. Young, *The Technical Writer's Handbook* (G—Reference Information and Interdisciplinary Subjects Series). Melville, NY, USA: Univ. Science Books, 2002.

[11] M. Rogge, A. Larsen, and D. U. Sauer, "Electrification of public transport bus fleets with battery electric buses: Development of a software toolchain for the changeover planning of entire bus fleets with consideration of technical and operational constraints," RWTH Publications, Aachen Univ., Aachen, Germany, Tech. Rep., 2020, doi: 10.18154/RWTH-2021-02146.

[12] R. Schreiber. (2022). *Market Analysis: Electric Buses Keep Booming in Europe*. Accessed: May 30, 2022. [Online]. Available: https://www.electrive.com/2022/03/01/market-analysis-electric-buses-keep-booming-in-europe/

[13] BloombergNEF. (2022). *Battery Pack Prices Fall to an Average of 132 $/kWh, But Rising Commodity Prices Start to Bite*. Accessed: Jun. 7, 2022. [Online]. Available: https://about.bnef.com/blog/battery-pack-prices-fall-to-an-average-of-132-kwh-but-rising-commodity-prices-start-to-bite/

[14] A. Hoke, A. Brissette, K. Smith, A. Pratt, and D. Maksimovic, "Accounting for lithium-ion battery degradation in electric vehicle charging optimization," *IEEE J. Emerg. Sel. Topics Power Electron.*, vol. 2, no. 3, pp. 691–700, Sep. 2014, doi: 10.1109/JESTPE.2014.2315961.

[15] V. Conti, S. Orchi, M. P. Valentini, M. Nigro, and R. Caló, "Design and evaluation of electric solutions for public transport," *Transp. Res. Proc.*, vol. 27, pp. 117–124, Jan. 2017, doi: 10.1016/j.trpro.2017.12.033.

[16] S. Deb, "Charging demand prediction for public electric city buses of Helsinki, Finland by support vector machine," in *Proc. 2nd Int. Conf. Power Electron. IoT Appl. Renew. Energy Control (PARC)*, Jan. 2022, pp. 1–6, doi: 10.1109/PARC52418.2022.9726683.

[17] N. Janjamraj, N. Changsarn, and S. Hiranvarodom, "Design of traction motor and battery for the modification of old BMTA public bus to e-bus," in *Proc. 9th Int. Electr. Eng. Congr. (iEECON)*, Mar. 2021, pp. 101–104, doi: 10.1109/iEECON51072.2021.9440335.

[18] L. S. Ashkezari, H. J. Kaleybar, M. Brenna, and D. Zaninelli, "E-bus opportunity charging system supplied by tramway line: A real case study," in *Proc. IEEE Int. Conf. Environ. Electr. Eng. IEEE Ind. Commercial Power Syst. Eur. (EEEIC/ICPS Europe)*, Jun. 2022, pp. 1–6, doi: 10.1109/EEEIC/ICPSEurope54979.2022.9854598.

[19] C. Beckers, I. Besselink, and H. Nijmeijer, "On-line test of a real-time velocity prediction for E-bus energy consumption estimation," in *Proc. IEEE Vehicle Power Propuls. Conf. (VPPC)*, Oct. 2021, pp. 1–5, doi: 10.1109/VPPC53923.2021.9699205.

[20] M. A. Shihab, S. F. Contreras, N. Mohseni, and J. Myrzik, "Optimal planning algorithm for a coordinated E-bus charging infrastructure," in *Proc. CIRED Porto Workshop, E-Mobility Power Distrib. Syst.*, Jun. 2022, pp. 696–700, doi: 10.1049/icp.2022.0799.

[21] N. Rodrigues, S. Thakare, S. Vyas, and R. Kumar, "Optimized charge scheduling of electric buses in a city bus network," in *Proc. IEEE Int. Conf. Power Electron., Drives Energy Syst. (PEDES)*, Dec. 2020, pp. 1–6, doi: 10.1109/PEDES49360.2020.9379431.

[22] C. Zhang, "Research on optimal configuration model of city's bus route electrification," in *Proc. IEEE Conf. Energy Internet Energy Syst. Integr. (EI2)*, Nov. 2017, pp. 1–6, doi: 10.1109/EI2.2017.8245400.

[23] C. Zhang, J. Tao, and Y. Cheng, "Research on optimal electrification selection and sequence scheme model of city's bus routes," in *Proc. IEEE Conf. Energy Internet Energy Syst. Integr. (EI2)*, Nov. 2017, pp. 1–6, doi: 10.1109/EI2.2017.8245556.

[24] G. Valenti, C. Liberto, M. Lelli, M. Ferrara, M. Nigro, and C. Villante, "The impact of battery electric buses in public transport," in *Proc. IEEE Int. Conf. Environ. Electr. Eng. IEEE Ind. Commercial Power Syst. Eur. (EEEIC/ICPS Europe)*, Jun. 2017, pp. 1–5, doi: 10.1109/EEEIC.2017.7977517.

[25] C. Liberto, G. Valenti, S. Orchi, M. Lelli, M. Nigro, and M. Ferrara, "The impact of electric mobility scenarios in large urban areas: The Rome case study," *IEEE Trans. Intell. Transp. Syst.*, vol. 19, no. 11, pp. 3540–3549, Nov. 2018, doi: 10.1109/TITS.2018.2832004.

[26] G. Desaulniers and M. D. Hickman, "Public transit," in *Handbooks in Operations Research and Management Science*, vol. 14. Amsterdam, The Netherlands: Elsevier, Feb. 2007, ch. 2, pp. 69–127, doi: 10.1016/S0927-0507(06)14002-5.
[27] J. R. Daduna and J. M. P. Paixão, "Vehicle scheduling for public mass transit—An overview," in *Computer-Aided Transit Scheduling*. Berlin, Germany: Springer, 1995, pp. 76–90.
[28] A. Haghani and Y. Shafahi, "Bus maintenance systems and maintenance scheduling: Model formulations and solutions," *Transp. Res. A, Policy Pract.*, vol. 36, no. 5, pp. 453–482, 2002, doi: 10.1016/S0965-8564(01)00014-3.
[29] J. Békési, B. Dávid, and M. Krész, "Integrated vehicle scheduling and vehicle assignment," *Acta Cybern.*, vol. 23, no. 3, pp. 783–800, 2018, doi: 10.14232/actacyb.23.3.2018.4.
[30] D. Vujanovic, V. Momcilovic, and M. Vasic, "A hybrid multi-criteria decision making model for the vehicle service center selection with the aim to increase the vehicle fleet energy efficiency," *Thermal Sci.*, vol. 22, no. 3, pp. 1549–1561, 2018, doi: 10.2298/TSCI170530208V.
[31] D. Vujanovic, V. Momcilovic, and O. Medar, "Influence of an integrated maintenance management on the vehicle fleet energy efficiency," *Thermal Sci.*, vol. 22, no. 3, pp. 1525–1536, 2018, doi: 10.2298/TSCI170209122V.
[32] *Technical Report R4 Submitted to IESO Conservation Fund, Optimization toolbox for Public Bus Transit Electrification*, Dept. Elect. Eng. Comput. Sci., Smart-Grid Res. Lab, Lassonde School Eng., York Univ., Toronto, ON, Canada, 2020.
[33] Phyphox. (2016) *Phyphox-Physical Phone Experiments*. [Online]. Available: https://phyphox.org/
[34] (2018). *MATLAB and Simulink Racing Lounge: Vehicle Modeling, MathWorks Student Competitions Team*. [Online]. Available: https://it.mathworks.com/matlabcentral/fileexchange/63823-MATLAB-and-simulink-racing-lounge-vehicle-Modeling and https://github.com/mathworks/vehicle-modeling/releases/tag/v4.1.1
[35] S. Heydari, P. Fajri, M. Rasheduzzaman, and R. Sabzehgar, "Maximizing regenerative braking energy recovery of electric vehicles through dynamic low-speed cutoff point detection," *IEEE Trans. Transport. Electrific.*, vol. 5, no. 1, pp. 262–270, Mar. 2019.
[36] E. D. Kostopoulos, G. C. Spyropoulos, and J. K. Kaldellis, "Real-world study for the optimal charging of electric vehicles," *Energy Rep.*, vol. 6, pp. 418–426, Nov. 2020, doi: 10.1016/j.egyr.2019.12.008.
[37] Q. Chen, S. Kang, H. Chen, Y. Liu, and J. Bai, "Acceleration slip regulation of distributed driving electric vehicle based on road identification," *IEEE Access*, vol. 8, pp. 144585–144591, 2020, doi: 10.1109/ACCESS.2020.3014904.
[38] C. Leone, G. Piazza, M. Longo, and S. Bracco, "Electrification of LPT in Algeciras Bay: A new methodology to assess the consumption of an equivalent e-bus," *Energies*, vol. 14, no. 16, p. 5117, Aug. 2021, doi: 10.3390/en14165117.
[39] B. J. Varocky, H. Nijmeijer, S. T. H. Jansen, I. I. Besselink, R. C. Mansvelder, and R. R. Mansvelders, "Benchmarking of regenerative braking for a fully electric car," D&C, Eindhoven Univ. Technol., Eindhoven, The Netherlands, 2011, vol. 2011.002.
[40] A. Khanipour, K. M. Ebrahimi, and W. J. Seale, "Conventional design and simulation of an urban hybrid bus," *World Acad. Sci., Eng. Technol., Int. J. Mech., Aerosp., Ind., Mechtron. Manuf. Eng.*, vol. 01, pp. 146–152, Aug. 2007.
[41] T. Paul and H. Yamada, "Operation and charging scheduling of electric buses in a city bus route network," in *Proc. 17th Int. IEEE Conf. Intell. Transp. Syst. (ITSC)*, Oct. 2014, pp. 2780–2786, doi: 10.1109/ITSC.2014.6958135.

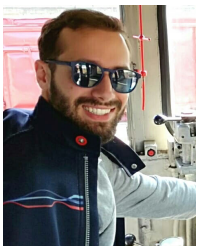

ANDREA DI MARTINO received the M.Sc. degree in mechanical engineering from Politecnico di Milano, Milan, Italy, in 2020, where he is currently pursuing the Ph.D. degree in electrical engineering. His research interests include mobility, transportation systems, and electric vehicles and traction. He is a member of the Italian Group of Engineering about Railways (CIFI).

GAURI SHANKAR PRASAD received the B.Sc. degree in mechanical engineering from the Indian Institute of Technology, India, in 2019, and the M.Sc. degree in mobility engineering from Politecnico di Milano, Milan, Italy, in 2022.

FEDERICA FOIADELLI (Senior Member, IEEE) received the M.Sc. and Ph.D. degrees in electrical engineering from Politecnico di Milano, Milan, Italy, in 2003 and 2008, respectively. She is currently an Associate Professor with the Department of Energy, Politecnico di Milano. Her research interests include electric power systems and electric traction. She is a member of the Italian Group of Engineering about Railways (CIFI) and the Italian Electric Association (AEIT).

MICHELA LONGO (Member, IEEE) received the M.Sc. degree in information engineering and the Ph.D. degree in mechatronics, information, innovative technologies and mathematical methods from the University of Bergamo, Bergamo, Italy, in 2009 and 2013, respectively. She is currently an Associate Professor with the Department of Energy, Politecnico di Milano, Milan, Italy. Her research interests include electric power systems, electric traction, and mechatronics. She is a member of the Italian Group of Engineering about Railways (CIFI) and the Italian Electric Association (AEIT).

Open Access funding provided by 'Politecnico di Milano' within the CRUI CARE Agreement